New Astronomy 33 (2014) 26–37

Contents lists available at ScienceDirect

New Astronomy

journal homepage: www.elsevier.com/locate/newast

Geant4 software application for the simulation of cosmic ray showers in the Earth's atmosphere

P. Paschalis [a], H. Mavromichalaki [a,*], L.I. Dorman [b,c], C. Plainaki [a,d], D. Tsirigkas [a]

[a] Nuclear and Particle Physics Section, Physics Department, National and Kapodistrian University of Athens, 15784 Athens, Greece
[b] Israel Cosmic Ray & Space Weather Centre and Emilio Ségre Observatory, Tel Aviv University, Golan Research Institute, and Israel Space Agency, Israel
[c] Cosmic Ray Department of N.V. Pushkov IZMIRAN, Russian Academy of Science, Moscow, Russian Federation
[d] INAF, Institute of Space Astrophysics and Planetology, Via del Fosso del Cavaliere 100, 00133 Rome, Italy

HIGHLIGHTS

- A new Geant4 software application-DYASTIMA- is presented.
- It can be used for the simulation of atmospheric showers caused by cosmic rays.
- It is an easy to use application and can fit to a variety of other applications.
- It can easily be parameterized in several parts.
- It fits many needs, as the cosmic ray spectrum, the atmospheric structure and the magnetic field.

ARTICLE INFO

Article history:
Received 1 December 2013
Received in revised form 20 March 2014
Accepted 25 April 2014
Available online 6 May 2014
Communicated by W. Soon

Keywords:
Cosmic rays
Atmosphere
Geant4
Simulation

ABSTRACT

Galactic cosmic rays and solar energetic particles with sufficient rigidity to penetrate the geomagnetic field, enter the Earth's atmosphere and interact with the electrons and the nuclei of its atoms and molecules. From the interactions with the nuclei, cascades of secondary particles are produced that can be detected by ground-based detectors such as neutron monitors and muon counters. The theoretical study of the details of the atmospheric showers is of great importance, since many applications, such as the dosimetry for the aviation crews, are based on it. In this work, a new application which can be used in order to study the showers of the secondary particles in the atmosphere is presented. This application is based on the Monte Carlo simulation techniques, performed by using the well-known Geant4 toolkit. We present a thorough analysis of the simulation's critical points, including a description of the procedure applied in order to model the atmosphere and the geomagnetic field. Representative results obtained by the application are presented and future plans for the project are discussed.

1. Introduction

Galactic cosmic rays (GCRs) are particles that originate from stellar sources and are accelerated to high energies. They consist mainly of protons (∼89%), alpha particles (∼10%) and a small portion (∼1%) of heavier nuclei. The energy spectrum of the cosmic rays is wide, ranging from about 10^9 eV to extremely high energies of about 10^{21} eV. However, the flux of the particles decreases rapidly as their energy increases; hence, common cosmic rays have energies from about 1 GeV to a few hundreds of GeV (Gaisser et al., 2001). The magnetic field of the Earth provides shielding of the planet from the cosmic ray particles. Depending on their rigidity, cosmic rays penetrate the magnetic field of the Earth and reach the top of the atmosphere (Smart et al., 2000). The insertion and penetration of cosmic rays in the Earth's atmosphere depend on the particle energy and incident velocity direction and are highly related to the solar activity. The solar wind conditions at 1 AU from the Sun, modulate the Earth's magnetic field and often modify the magnetic cut-off rigidity as well, allowing the entrance of lower energy particles in the atmosphere. Furthermore, during periods of intense solar activity, manifested by coronal mass ejections (CMEs) and solar flares, the cosmic ray flux at the vicinity of the Earth can be enhanced. This is due to solar energetic particles (SEPs) which arrive at the Earth and have a composition similar to that of the galactic cosmic rays and energies from a few keV to a few GeV (Miroshnichenko, 2001). These particles are also known as Solar Cosmic Rays (SCRs) and sometimes lead

* Corresponding author. Fax: +30 210 7276987.
E-mail address: emavromi@phys.uoa.gr (H. Mavromichalaki).

http://dx.doi.org/10.1016/j.newast.2014.04.009
1384-1076/

to Ground Level Enhancements (GLEs), where an increase of cosmic ray intensity is detected at ground level (Belov et al., 2005; Plainaki et al., 2005, 2007). However, the intense solar activity may often have the opposite result, reducing the galactic cosmic ray flux for 1 week and more, leading to Forbush decreases (Lockwood, 1971; Papaioannou et al., 2009).

As the cosmic ray particles enter the atmosphere, they interact with the electrons and the nuclei of its atoms and molecules and secondary particles are generated. These secondary particles interact further, through several processes, such as elastic and inelastic scattering, decay, pair production, annihilation, Compton scattering, photoelectric effect, ionization, Bremsstrahlung radiation and Cherenkov radiation. The result is showers of muons, neutrinos, electrons, positrons, gammas, as well as neutrons, protons, π+ and K+ (Dorman, 2004; Longair, 2011). Secondary cosmic rays are continuously monitored by ground-based detectors. Neutron monitors measure the hadronic component of the secondary cosmic rays (http://www.nmdb.eu), muon counters measure the muonic component, while Cherenkov detectors register the Cherenkov radiation produced by the passage of high energetic charged particles through the atmosphere. The study of the secondary particle showers is of great importance, since it provides a correlation between the secondary cosmic rays that are measured by the ground based detectors and the primary cosmic rays at the top of the atmosphere. This correlation is of particular importance, when ground-based measurements are used as inputs for space weather applications. Moreover, the study of the atmospheric showers contributes to the determination of the affection that the barometric pressure and the temperature have on the hadronic and the muonic cosmic ray components respectively (Kobelev et al., 2011; Paschalis et al., 2013a). The determination of the relation between barometric pressure/temperature and cosmic ray flux registered at ground-level is also very useful in the primary processing of the ground based detectors data. Finally, an important application of the cosmic ray showers study is the calculation of the radiation dose to which aircraft crews are exposed (Bütikofer and Flückiger, 2011).

An efficient way to study the cosmic ray showers is via Monte Carlo (MC) simulations, which are very useful tools for the representation of several physical phenomena. The MC simulation technique has been used several times in cosmic ray studies. Many of these studies make use of the well known FLUKA (Battistoni et al., 2007; Ferrari et al., 2005) and Geant4 (Agostinelli et al., 2003; Allison et al., 2006) simulation toolkits. The operation and the detection efficiency of the neutron monitors have been studied for several cases and from various aspects (Balabin et al., 2011; Maurchev et al., 2011; Semikh et al., 2012; Paschalis et al., 2013b). The interactions of cosmic ray particles with the matter of the Earth's atmosphere have also been studied via simulations (Battistoni et al., 2003; Desorgher et al., 2003), while the development of the CRII model which calculates the cosmic ray induced ionization in the atmosphere, is very important as well (Usoskin et al., 2004, 2010; Usoskin and Kovaltsov, 2006). The response and the yield function of a neutron monitor have also been investigated several times, with the MC simulation of the cosmic rays propagation through the atmosphere and their detection by the neutron monitor (Debrunner et al., 1982; Clem, 1999; Clem and Dorman, 2000; Flückiger et al., 2008; Matthiä et al., 2009; Mishev et al., 2013). Apart from these works, very important is the development of standalone programs for the simulation of the cosmic ray interactions with the matter of the atmosphere. Heck et al. (1998) have developed CORSIKA while a similar application, based on Geant4, is the ATMOCOSMICS (Desorgher et al., 2005). The ATMOCOSMICS is usually combined with MAGNETOCOSMICS, based also on Geant4, which determines the transport of the cosmic ray particles in the Earth's magnetosphere. Finally, PLANETOCOSMICS combines and extends MAGNETOCOSMICS and ATMOCOSMICS in order to study the propagation of the cosmic rays in several planets, such as Earth, Mars and Mercury (Desorgher et al., 2006; Dartnell et al., 2007; Gurtner et al., 2007).

In this work, the first version of a Dynamic Atmospheric Shower Tracking Interactive Model Application (DYASTIMA) for the simulation of cosmic ray showers in the atmosphere based on the Geant4 toolkit (Agostinelli et al., 2003; Allison et al., 2006), is presented. Two aims were primarily taken into account during the implementation of DYASTIMA. The first one was the development of an application, which can be easily parameterized in several points, in order to adapt to different conditions of atmospheric structure, magnetic field and primary cosmic ray spectrum. The second one was the provision of multiple output information in such a format that its direct insertion in several applications will be possible. This work is organized as follows: in Section 2 the model description is presented. In Section 3, we give some representative results and discuss their utility in other space weather applications. In Section 4, the main conclusions of this work and some future ideas are discussed.

2. Implementation steps

The implementation of DYASTIMA consists of three main parts: (a) the modeling of the environment that affects the cosmic ray showers, in such a manner, that the user can adapt it to his simulation scenario, (b) the determination of the simulation scenario in Geant4 and the use of the Geant4 for the simulation of the actual cascade and (c) the output of the simulation results, in such a way as to be easily used by a variety of applications. Geant4 is a well known simulation package written in C++ that was initially developed for the simulation of high energy physics and gradually got enhanced, in order to be applied to lower energies. The package provides a huge variety of options and great support through the official and unofficial web communities (http://geant4.cern.ch; http://hypernews.slac.stanford.edu/HyperNews/geant4/cindex). For all these reasons Geant4 is currently used for a variety of applications, not only in high energies (Banerjee et al., 1999; Costanzo et al., 2006; Apostolakis et al., 2008), but also in nuclear physics (Kaitaniemi et al., 2010; Heikkinen et al., 2010) and in medical physics (Rodrigues et al., 2004; Canadas et al., 2011). In the field of cosmic rays research, Geant4 has also been used as was mentioned in the introduction. In the following paragraphs, we describe the modeling of DYASTIMA, its implementation steps and its usage critical points.

2.1. Modeling

In order to implement a simulation of the cosmic ray propagation through the atmosphere, the following physical quantities and processes that affect the simulation should be modeled first:

- the spectrum of the primary cosmic rays that reach the top of the atmosphere
- the structure of the atmosphere
- the Earth's magnetic field
- the physics interactions that take place between the cosmic ray particles and the molecules of the atmosphere

These quantities are affected by various parameters, such as the space weather conditions, the current physical characteristics of the Earth's atmosphere, the time and the location for which the simulation is performed.

Apart from the physics of the interactions of the cosmic ray particles with the matter of the atmosphere that is described in the introduction and that does not depend on parameters that change, all the other quantities to be modeled depend on dynamic parameters. Beginning with the primary cosmic ray spectrum at the top of the atmosphere, as it has already been mentioned in the introduction, it depends on the solar activity. In order to represent the spectrum of particles at the top of the atmosphere, the parameterization of Papini et al. (1996) is used. According to this, the differential spectrum of the cosmic ray particles at the top of the atmosphere has the following form:

$$J(E) = A \cdot (E+B)^{a} \cdot E^{b} \quad \frac{particles}{m^2 \cdot sr \cdot s \cdot GeV/n} \tag{1}$$

where a, b, A, B are parameters that depend on the solar activity and E is the energy per nucleon of the particle. This parameterization is selected, since it includes the solar modulation at low energies, due to factor $(E+B)^{\alpha}$, while at higher energies the factor E^b dominates, leading to the well known exponential form.

The atmosphere is not a static system, as it is affected by the location and the time of the observation. It extends to an altitude of about 100 km above the surface of the Earth, where the Kalman line is located. The Kalman line is considered as the boundary between the atmosphere and the outer space, where collisions between particles are sparse. In general, the atmosphere is thinner over the poles and thicker over the equator, while for the same location, its accurate structure depends on several dynamic parameters. The accurate structure of the atmosphere is determined via the temperature profile with altitude. By using these profiles and by integrating the hydrostatic equation, the pressure and the density can be calculated in any altitude. Since the atmosphere is in the focus of several applications, especially in aviation, standard models that give a good approximation of the atmospheric structure, in most cases, have been constructed. These models are the US Standard Atmosphere (U.S. Government Printing Office, 1976) and the International Standard Atmosphere (International Civil Aviation Organization, 1993), which are identical up to 32 km from the surface.

Regarding the magnetic field of the Earth, it can be distinguished into two regions. In the inner region, the field (also named as geomagnetic field) is a superposition of the internal field and the crustal field, caused by electric currents in the Earth's core and magnetic regions in the Earth's crust respectively (International Association of Geomagnetism and Aeronomy, 2010). In the external region, the field (also named as magnetospheric field) is configured by the interaction of the internal field with the solar wind (Tsyganenko, 1989, 1995). The geomagnetic field dominates in the region up to ~4 Earth radii from the Earth's surface. Beyond this distance, the magnetospheric field dominates extending up to the magnetopause. In the simulation, the starting point of particles is the top of the atmosphere and the magnetic field is necessary in order to calculate the divergence of the tracks of the charged particles inside the atmosphere. Considering the fact that the atmosphere extends up to about 100 km above the Earth's surface, a sufficient approximation for the magnetic field up to this altitude is its representation by a magnetic dipole. Thus, if the magnetic field $\overrightarrow{B_0}$ on the ground is known, the magnetic field $\overrightarrow{B_h}$ at an altitude h is considered to be a nearly parallel vector with magnitude:

$$|\overrightarrow{B_h}| = |\overrightarrow{B_o}| \cdot \frac{r_{earth}^3}{(r_{earth}+h)^3} \tag{2}$$

According to Eq. (2), the decrease of the magnetic field's strength at the top of the atmosphere compared to its strength at the ground is about 4.5%. Eq. (2) does not consider that the magnetic dipole is located about 433 km off the Earth's centre and inclined 15° to the axis of rotation. However, the attenuation of the field through the atmosphere is so insignificant that this offset is not considered in the calculations, for simplicity reasons. The values of the magnetic field on ground level are known (www.ngdc.noaa.gov/geomag/).

2.2. Development of the application

According to the modeling described above, the simulation requires the determination of several settings. These settings are defined via external configuration files which contain the necessary variables concerning:

- the representation of the atmosphere and the magnetic field
- the primary particles that enter the atmosphere
- the physics interactions that take place
- the altitudes at which the tracking of particles will be performed
- the energy thresholds for the production, simulation and tracking of particles

Since Geant4 supports volumes made of materials with constant density and considering the fact that the density of the atmosphere decreases from the bottom to the top, the atmosphere of the Earth is represented with slices each one of which has a constant density. The division of the atmosphere is performed in such a manner that the change of the density from one slice to the next is smaller than a defined percentage. The number of the slices that the atmosphere is divided to, as a function of the density change between them is presented in Fig. 1. Two different geometry models have been implemented for the atmosphere. The first one corresponds to a flat atmosphere in which the slices are rectangular boxes. The other model corresponds to a spherical model which takes into account the curving of the Earth and, as a result, the slices are considered as spherical shells. For each model, a non uniform magnetic field is created with a magnitude that attenuates with altitude according to Eq. (2). Below the slices of the atmosphere, a slice that represents the Earth's surface, land or sea, may be added in order to simulate the interactions of the shower with the surface.

The primary particles are emitted from a point source at the top of the atmosphere. The energies of the primary particles follow the spectrum of Eq. (1) and are inside user defined limits. The zenith and the azimuth incident direction of the particles are also inside user defined limits. The angular distribution of the emitted particles follows a cosine-law distribution which represents the distribution seen at a plane from a uniform 2p flux (Lambert's cosine law). The particle beam may consist of several particle types with

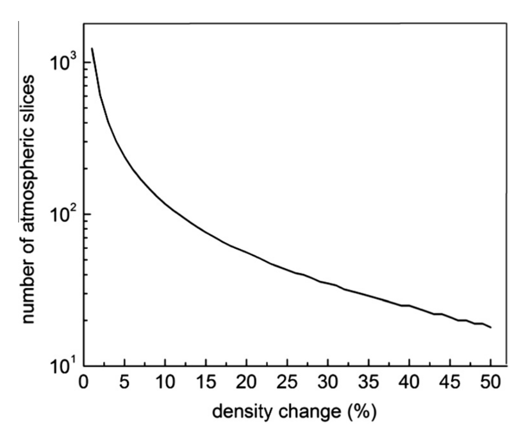

Fig. 1. The number of the atmospheric slices as a function of the density change between them. A steep increase of the slices' number is noticed below 10%.

defined relative abundances. Referring to the physics interactions, Geant4 provides a great variety of physics processes each one of which is realized via several models. The Geant4 application developer is encouraged to build his own physics list, which should take into account the necessary for the simulation processes and the optimal models. However, Geant4 provides several reference physics lists which have been constructed through the experience and the validation of other experiments. DYASTIMA makes use of these reference physics lists, since most of them cover all the physics interactions that take place in the development of the particles shower. As the simulation is performed, the application collects two types of information. The first one concerns the secondary particles at the time of their generation while the other one concerns the particles that cross user defined atmospheric altitudes (tracking layers).

A critical point that should be considered is the energy thresholds above which the particles are produced, simulated and tracked (energy cuts). DYASTIMA provides the corresponding three types of energy thresholds. The first type of energy threshold, acts only to the production of secondary particles. The energy of a particle that is going to be produced is checked by the application and if it is below the defined threshold its production is rejected. A similar action is performed by using Geant4's range cut feature. According to it, only particles with a range greater than a defined value are produced. The range cut is transformed by Geant4 into an energy threshold, taking into account the particle type and the medium in which it moves. In general, the reference physics lists of Geant4 have a default range cut of 1 mm for all particles and the application allows the modification of this value. It must be highlighted that the production energy threshold and the range cut feature refer only to the production of particles and not to their further simulation. After a particle is generated, it is simulated down to zero energy. The second and the third type of energy thresholds concern the energy values below which the particles are excluded from the simulation and the tracking respectively. The elimination of particles from the simulation or the tracking is performed by checking their energy at each simulation step, which is defined as the distance between two sequential interactions.

2.3. Inputs and outputs

Following the previous analysis, the user should define several parameters. Special attention should be given to the following settings:

- the parameters of the particles' beam
- the selection between the flat and the spherical model of the atmosphere
- the density change between the atmospheric slices
- the selection of the reference physics list
- the energy thresholds

Regarding the beam, the user should define the particles it consists of, their relative abundances, the parameters of their energy spectrums and the limits for their energy and for their zenith and azimuth directions. Papini et al. (1996) give values for the parameters of the spectrum, for the case of solar minimum and solar maximum activity which the user can use as a reference. In the special case that a monoenergetic beam with constant incident direction is to be studied, the user should set the minimum values of energy, zenith and azimuth, to be equal to the maximum ones. The optimal selection of the atmospheric model depends on the zenith angle of the incoming particles. In case the zenith angle of the incoming particles is small the flat model is sufficient, while in cases of great zenith angles the curviness of the Earth becomes important and the user should select the spherical model. About the density change, a value between 5% and 10% results to the division of the atmosphere to a few hundred slices which is considered optimal. Finally, the high energy of the incoming cosmic ray particles and the wide energy range of the secondary particles imply the use of a reference physics list optimal for high energy physics. Moreover, the use of a physics list that includes the NeutronHP model (physics lists ending in _HP) is considered optimal, as it handles more accurately the inelastic scattering of neutrons, which affects significantly the production of secondary particles. Thus, optimal reference physics lists for the simulation are considered to be, the QGSP_BIC_HP, QGSP_BERT_HP and FTFP_BERT_HP. These physics lists include all the well known processes such as ionization, photoelectric effect, Bremsstrahlung, Coulomb scattering, Compton scattering, pair production, annihilation, decay, capture, fission, hadronic elastic and inelastic scattering. These physics lists differ in the models that handle the inelastic scattering of hadrons. A comparison of these physics lists can be found in Paschalis et al. (2013b).

The determination of the energy thresholds is necessary in order to reject from the simulation the particles with very low energies that do not add relevant information in the context of the considered processes in this application. The setting of a range cut provides an easy and efficient way to reject the production of particles, without the need to define separate production thresholds for every possible particle type by the user. However, the user should consider that since the density of the atmosphere is reduced with altitude, the setting of a range cut leads to the determination of different energy thresholds for the production of particles at each altitude. If this is not desired, then constant production energy thresholds should be defined for each particle type separately. Regarding the energy thresholds for the simulation, the user should take into account that the generation of specific particles is affected by the elimination of its parent particles. Finally, the energy thresholds for the tracking do not affect the accuracy of the simulation, but only the collected information.

The input parameters, such as the number of the tracking layers, the number of the slices that the atmosphere is divided to, the use of the flat or the spherical model, may affect the accuracy of the simulation with a trade off to performance. However, the most critical parameters that affect the performance are expected to be the energy of the incident particle and the energy cuts of the secondary particles. Especially the energy cuts of that particles that are populous in the shower, influence the time performance often by orders of magnitude. Some comparable results of the performance when DYASTIMA runs on a mid range computer are shown in Fig. 2. The tests were performed by using vertical monoenergetic proton beams which are the most abundant primary cosmic ray particles. The physics list used was the QGSP_BIC_HP and the range cut of the particles was set to 1 m. We note that the use of the spherical model increases the required time for the simulation by about 50%. Moreover, it is concluded that the number of tracking layers does not affect the performance. On the other hand, the number of the slices that the atmosphere is divided to, affects slightly the performance when the energy of the incident protons is about 1 GeV. When the energy of the protons is greater, the number of slices does not affect the performance at all, probably because the performance is dominated by the huge number of secondary particles. However, as expected, the performance is majorly affected by the energy of the incident particle. The simulation time increases three orders of magnitude when the energy increases from 1 to 1000 GeV. At these energies the number of secondary particles becomes huge and in order for the simulation to be finished in a reasonable time, the accuracy should be manually reduced. The histogram of Fig. 2 shows how the range cut can

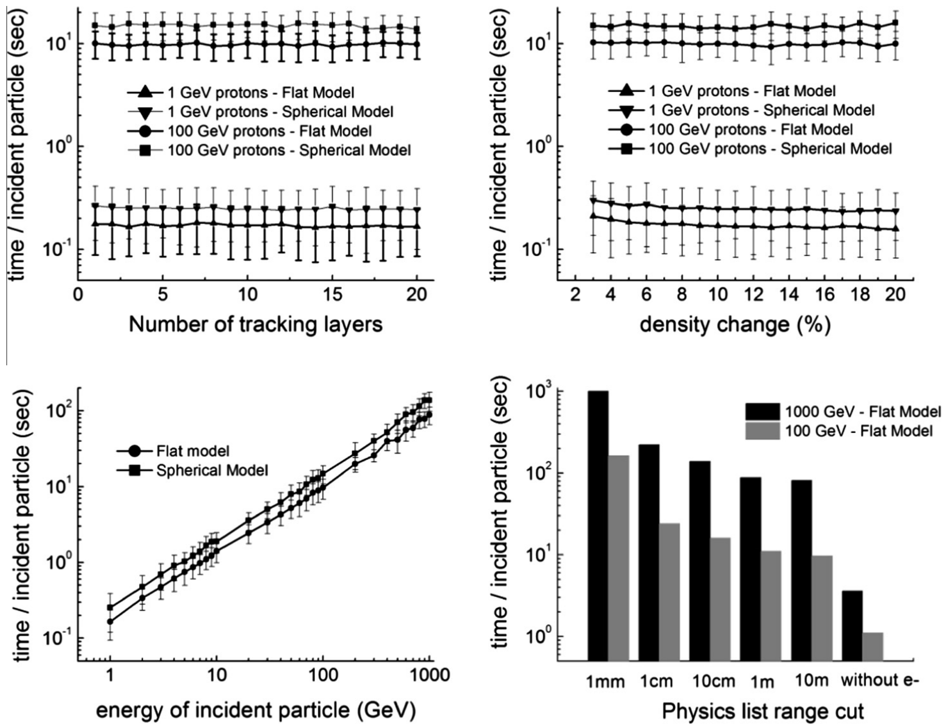

Fig. 2. Performance of the application using the QGSP_BIC_HP physics list with 1 m range cut. In the upper left panel, the number of tracking layers seems not to affect the performance regardless the energy of the incident particle. In the upper right panel, the density change between the slices affects slightly the performance for the low energy particles. In the lower left panel, the required time for the simulation increases orders of magnitude with the energy of the incoming particle. In the lower right panel, the range cut of the physics list can reduce the required time several orders of magnitude. The elimination of particles can further increase the performance.

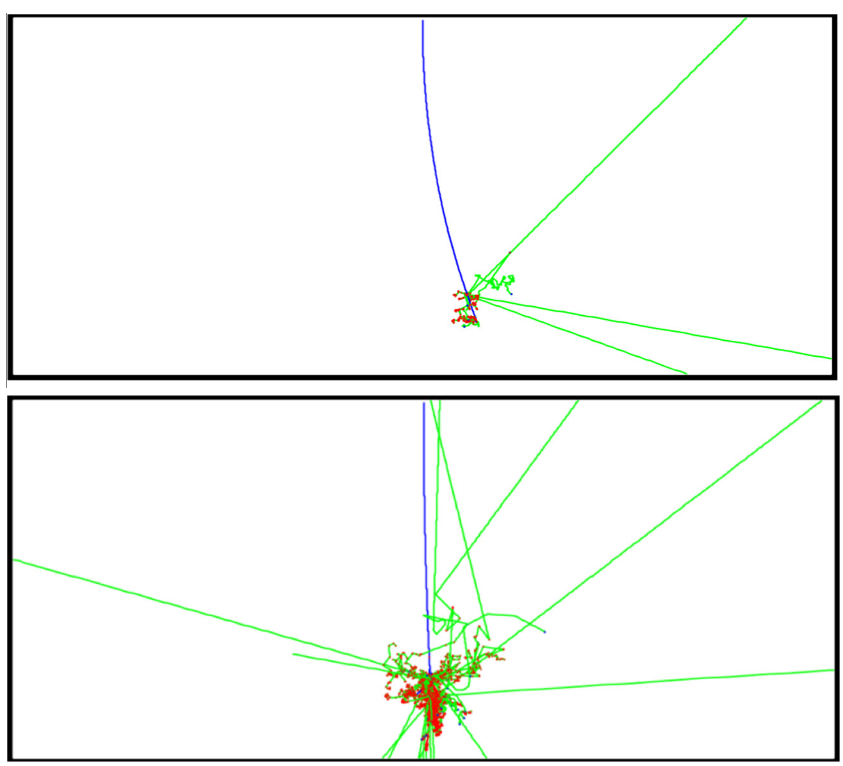

Fig. 3. Shower representation of a vertical proton with 1 GeV (up) and 10 GeV (down). Blue lines represent positive charge, red lines negative charge and green lines neutral. The shower's dimension increases with the energy increase. It is noticed the divergence of the track of the incoming proton, due to the magnetic field. The divergence decreases with the energy increase due to the velocity increase of the particle. (For interpretation of the references to color in this figure legend, the reader is referred to the web version of this article.)

reduce the required time for the simulation. Furthermore, the user may accelerate the simulation by adding additional energy cuts to specific particles such as the electrons.

The data that DYASTIMA collects are exported in .csv files in order for their further process. Regarding the secondary particles at the time of their production, the altitude of the production

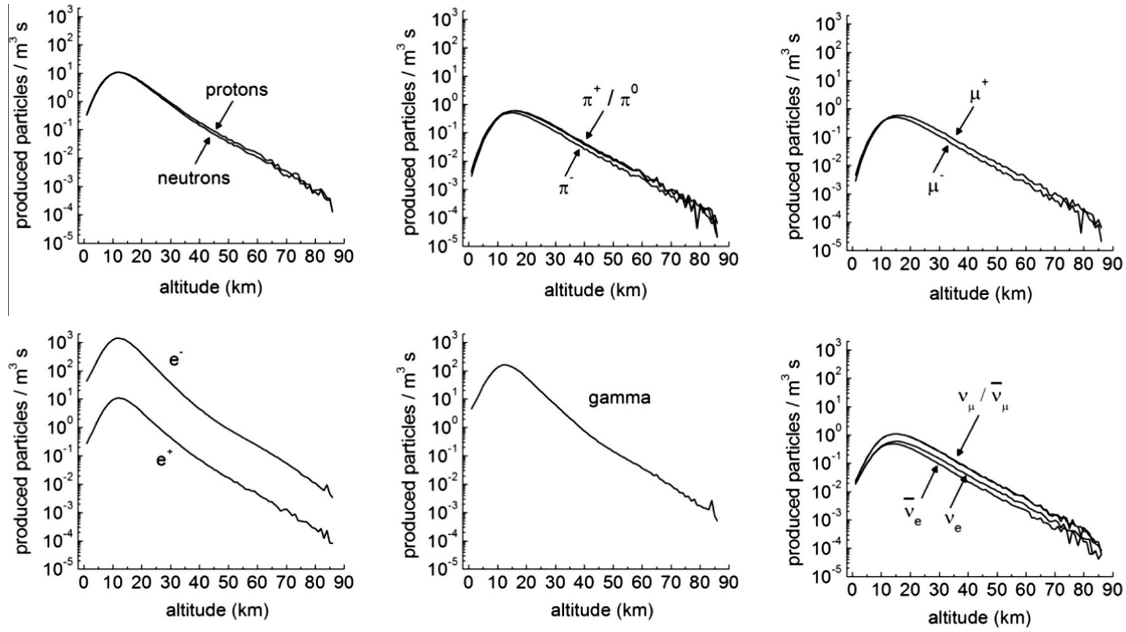

Fig. 4. The number of produced protons/neutrons, pions, muons, electrons, gamma and neutrinos when an 1 m range cut is used with respect to the altitude. The production presents a maximum at 10–20 km altitude, while e^- and gammas are the most populous due to the low energy particles resulted from ionization, Compton effect, photoelectric effect and Bremsstralung.

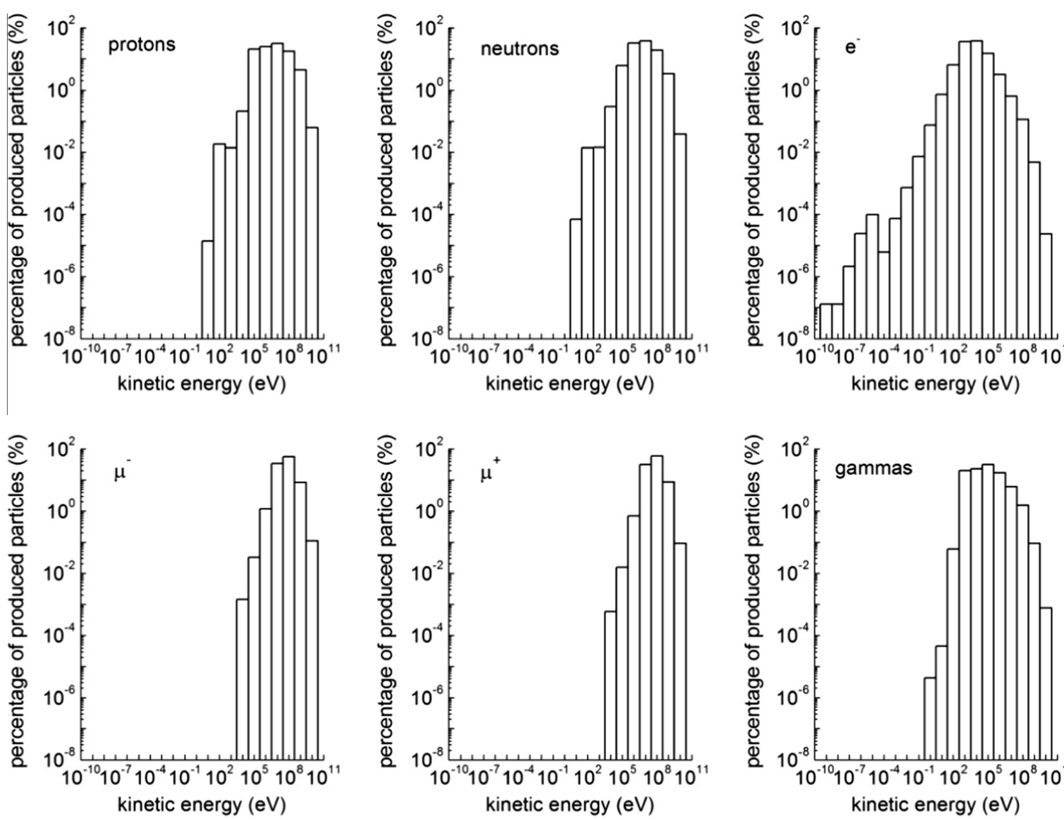

Fig. 5. Kinetic energy distribution of produced protons, neutrons, e^-, μ^-, μ^+, gammas when an 1 m range cut is used. The spectrum of e^- and gammas starts from very low energies due to ionization, Compton effect, photoelectric effect and Bremsstralung.

and the energy are registered. Regarding the tracking of particles at each tracking altitude, the energy, the direction, the horizontal position and the time are registered. Two output modes are provided. The first one corresponds to an analytic output in which a record is registered for each particle that is produced or tracked. The second one corresponds to a synoptic output in which the results are stored and processed after the whole simulation is finished. The synoptic output provides combined information about

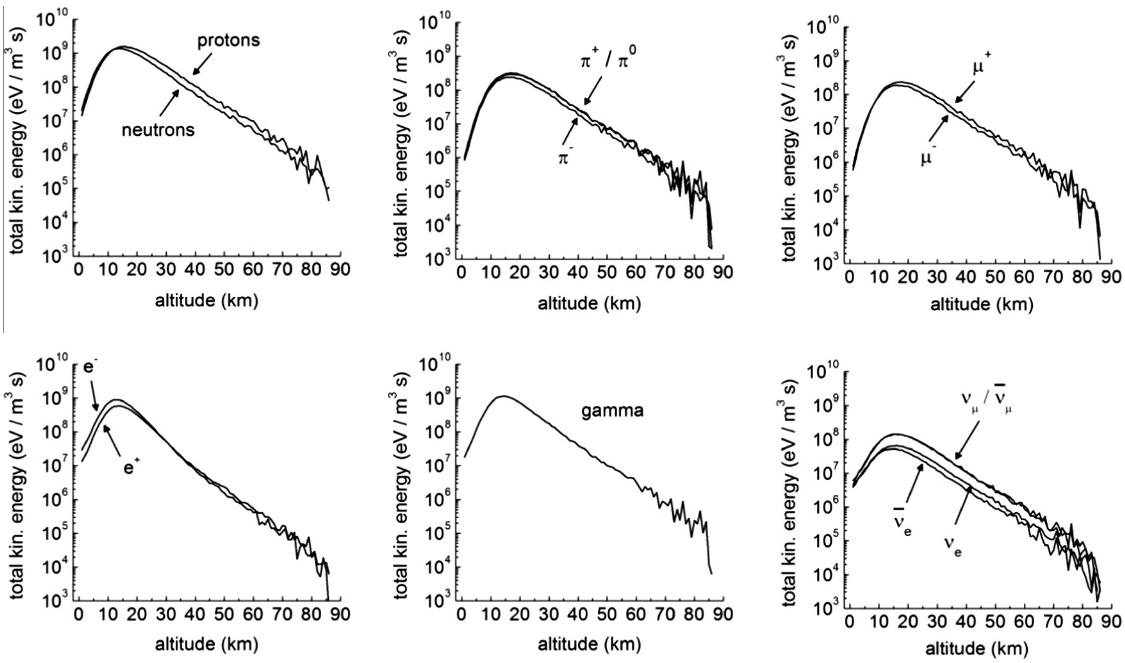

Fig. 6. Total kinetic energy of produced protons, neutrons, pions, muons, electrons, gamma and neutrinos when an 1 m range cut is used. Although the number of electrons and gammas is one to two orders of magnitude greater than the other particles (according to Fig. 4), their contribution to energy is similar with the contribution of the other particle types since a great portion of them correspond to particles with very low energies.

the simulation and can be used for the generation of plots. Finally, DYASTIMA provides a graphical representation of the geometry where a .heprep file is generated that can be viewed by the HEPREP viewer (http://www.slac.stanford.edu/~perl/heprep/index.html). A graphical representation of the simulation when a proton vertically enters the atmosphere is shown in Fig. 3, where the blue lines correspond to positive charge, the red lines to negative charge and the green lines to neutral charge. In the case of 1 GeV proton (upper panel), one can notice the divergence of the particle trajectory due to the magnetic field. In the case of 10 GeV protons (lower panel) the divergence is smaller due to the higher proton energy. We note that in case of greater incident proton energy the size of the particle shower is greater, as well.

3. Results and discussion

In this section some representative results of DYASTIMA are presented and discussed. The results are obtained by using the primary spectrum presented in Beringer et al. (2012). This spectrum consist of protons according to Shizake et al. (2007) and electrons/positrons according to measurements from several experiments. The corresponding plot from Beringer et al. (2012) was digitized and the parameters of equation (1) were adapted in order to fit the spectrums. The zenith angle of the incoming particles is set between 0° and 70° and the azimuth angle between 0° and 360°. The physics list used is the QGSP_BIC_HP which was selected as the most optimal for the simulation of the neutron monitor in Paschalis et al. (2013b). The range cut of the physics list is set to 1 m in order to avoid the production of particles with very low energies. The spherical model of the atmosphere is used with a structure representing the International Standard model, while the magnetic field values represent the Athens station location.

The first information that DYASTIMA provides, concerns the secondary particles at the time of their production. A great variety of particles and unstable nuclei are produced, however, only the results of some particle types are presented. Fig. 4 shows how many protons, neutrons, pions, muons, electrons, gamma and neutrinos are produced at each altitude. As it can be noticed, the production of the particles has a peak at 10–20 km above the Earth's surface. This result is consistent with previous studies (e.g. Usoskin et al., 2011) which argue that at this altitude the direct ionization by primaries is small, with the bulk ionization originating from the atmospheric cascade. The majority of the particles are electrons and gammas with protons and neutrons following. Pions and muons are of a similar population, while significant is the number of neutrinos. The absolute number of particles does not provide enough information since it is highly dependent on the production range cut. A range cut greater than 1 m will eliminate the production of the very low energy particles, reducing significantly the number of counted particles. For this reason it is

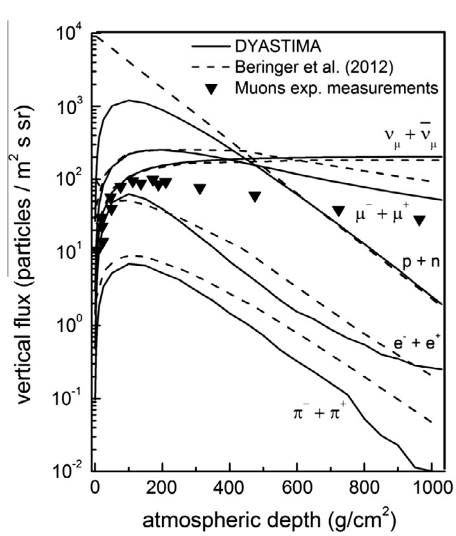

Fig. 7. The vertical flux of particles with energy >1 GeV that crosses each altitude in comparison to the results of Beringer et al. (2012). The comparison validates the results of DYASTIMA.

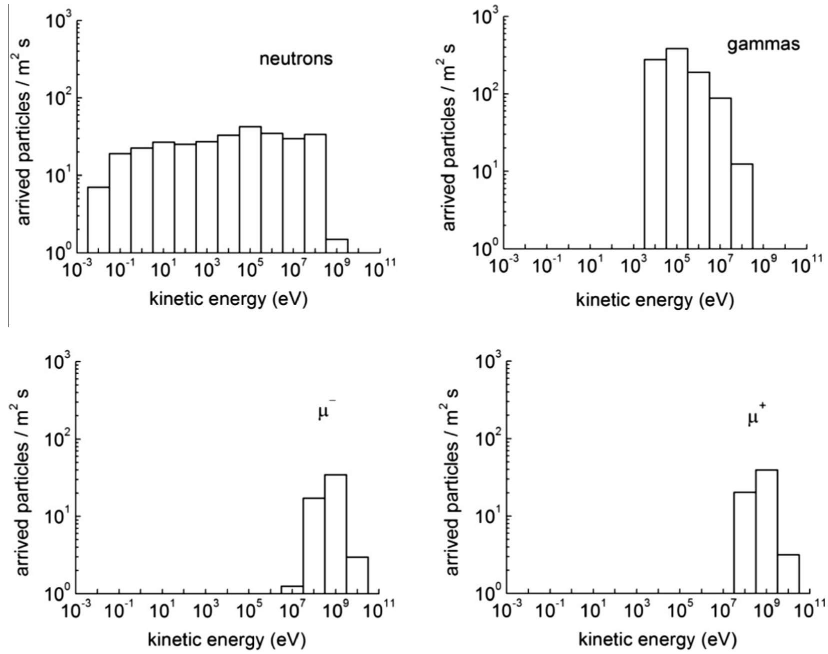

Fig. 8. Kinetic energy of neutrons, gammas and muons that arrive at sea level.

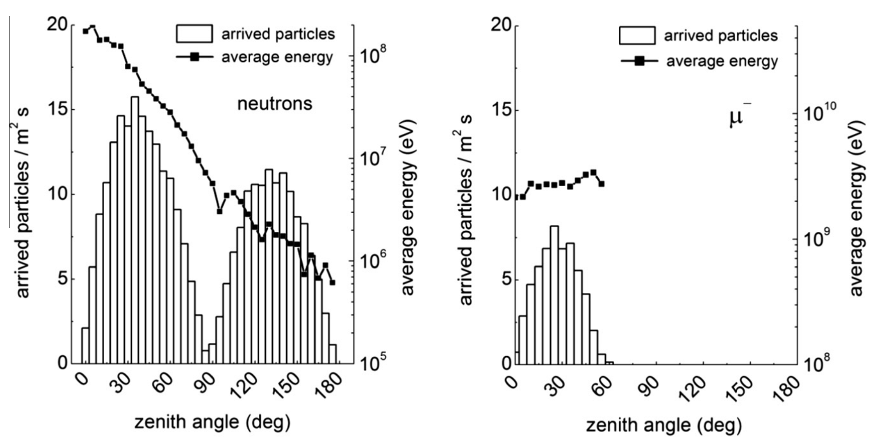

Fig. 9. The zenith angle distribution of neutrons that arrive at sea level and the corresponding average energy for each direction (left panel) present that the upward moving neutrons, resulted of elastic scatterings, have significantly smaller energies. The corresponding figure for μ^- (right panel) shows that all the particles are moving downward and their average energy does not depend on the direction.

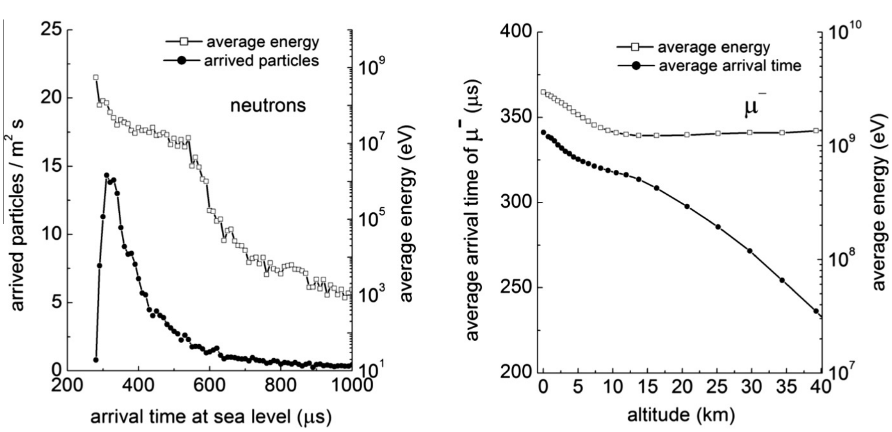

Fig. 10. The arrival time distribution of neutrons at sea level and the corresponding energy are presented in the left panel. Most neutrons arrive 350 μs after the primary cosmic ray particle enters the atmosphere; however, there are slower neutrons that arrive much later. The average arrival time and the average energy of the μ^- with respect to the altitude are presented in the right panel.

important to study the energy distribution of the secondary particles and give special attention to low energy particles. This information is provided by DYASTIMA and is presented in Fig. 5. Protons and neutrons share a similar distribution with energies in the zone of 10^1–10^{10} eV, while the majority of particles have energies with magnitude 10^5–10^9 eV. Negative and positive muons also share a similar spectrum with energies in the zone of 10^4–10^{10} eV, while the majority of particles have energies with magnitude 10^7–10^9 eV. The spectrum of gamma starts from low energies as a result of Bremsstrahlung, however the majority of gamma has energies with magnitude 10^3–10^8 eV. On the other hand, electrons have a wide spectrum starting from 10^{-9} eV, however, the majority of produced electrons have energies with magnitude 10^2–10^5 eV. The low energy electrons are the result of the propagation of gammas and of charged particles through the atmosphere. The gammas lose their energies due to Compton effect and are eventually absorbed due to the photoelectric effect while the charged particles, including the electrons, ionize the matter. The result of these processes is the production of electrons with very low energies. Fig. 6 provides combined information of the previous two figures and presents the total kinetic energy of the secondary particles that are produced at each altitude. It is noticed that although the number of electrons and gamma is one to two orders of magnitude greater than the other particles (according to Fig. 4), their contribution to energy is similar with the contribution of the other particle types, since a great portion of them correspond to particles with very low energies.

The previous figures correspond to the secondary particles at the time of their production. What is more important in practice is the number of particles that are detected at each altitude. It should be highlighted that the number of particles that are detected at each altitude differs from the number of particles that are produced at the same altitude (as shown in Fig. 4) since the high energetic secondary particles can travel long distances. The number of particles that is detected at each altitude can be accessed by DYASTIMA by defining several tracking layers distributed into the atmosphere. The number of the particles that are detected at each altitude is shown in Fig. 7. In order to compare the results with the ones presented in Beringer et al. (2012), the number of particles with energies greater than 1 GeV and with vertical direction is presented. It is noticed that the results are in agreement with Beringer et al. (2012). The vertical flux in general is greater at atmospheric depth of around 100 g/cm^2 (about 16 km altitude). At this altitude the flux of protons/neutrons is greater, with the flux of muons and neutrinos following. The flux of all particles decreases when approaching sea level. At an atmospheric depth of around 450–500 g/cm^2 (about 6 km altitude) the flux of protons/neutrons becomes smaller than the flux of neutrinos and muons, while at sea level neutrinos are the most abundant followed by muons. The fluxes of electrons/positrons and pions are

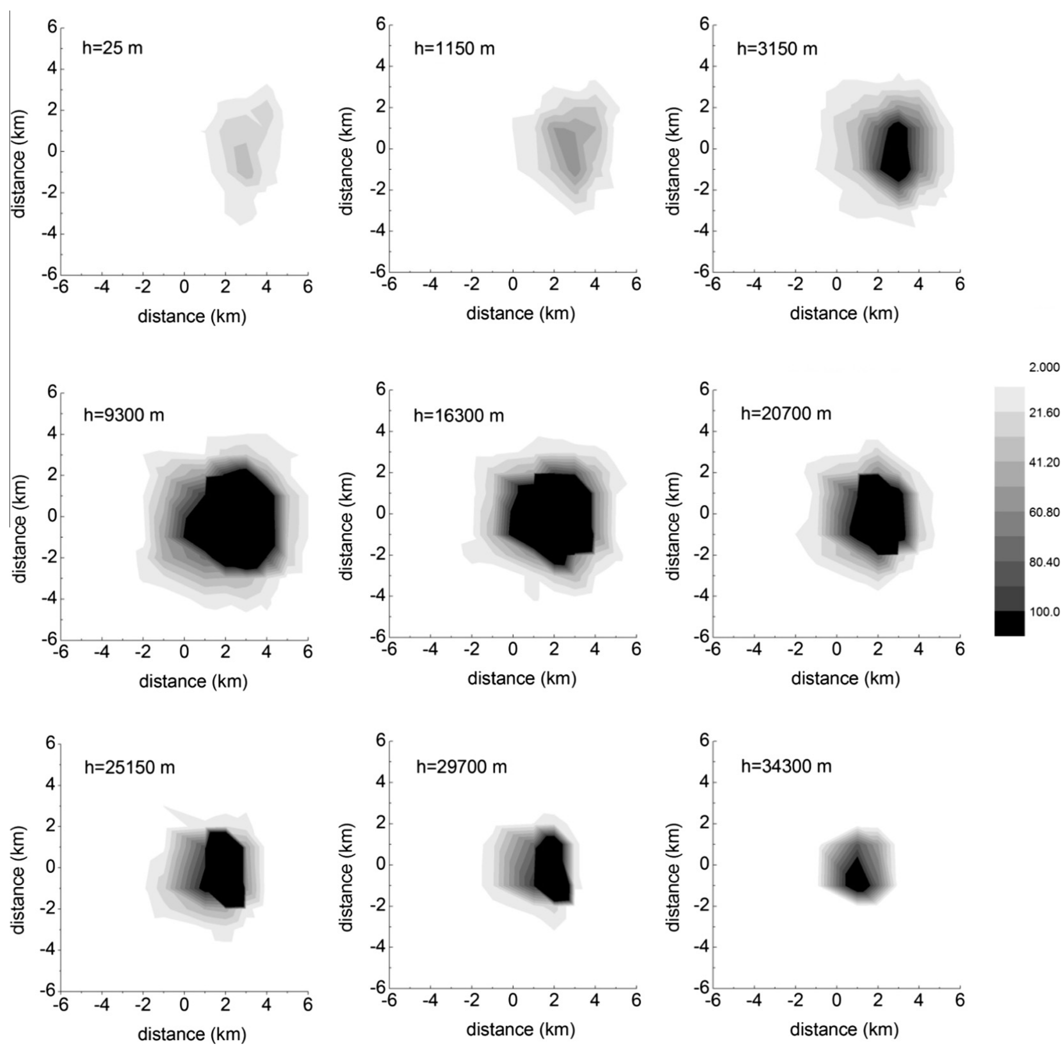

Fig. 11. Spatial distribution of the muons μ^- at different altitudes when a vertical 10 GeV proton beam enters the atmosphere. The shower has a dimension of about 8×8 km at an altitude of about 10 km.

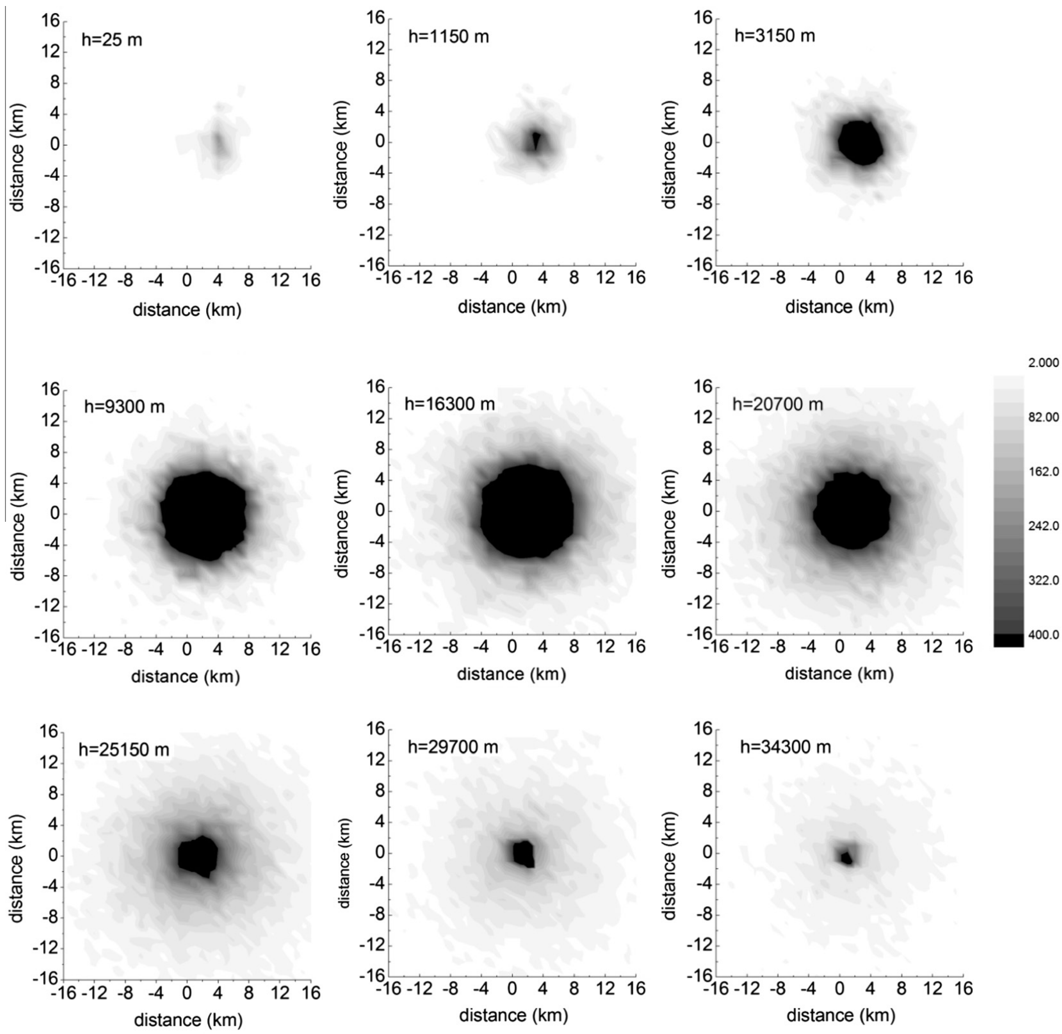

Fig. 12. Spatial distribution of neutrons at different altitudes when a vertical 10 GeV proton beam enters the atmosphere. The shower has a double dimension compared to that of μ^- and the maximum is presented at 16 km altitude.

smaller than the rest of the particles at all altitudes. It should be highlighted that the results of proton/neutrons and neutrinos are almost identical to Beringer et al. (2012). The small proton/neutron flux at the small atmospheric depth is due to the fact that only particles with energy greater than 1 GeV are presented. The majority of the primary protons have energies up to a few GeV and lose rapidly their energy, due to ionization, as they enter the atmosphere. As a result, their energy become less than 1 GeV and the particles are not included in Fig. 7. On the other hand, the calculated flux of muons is the same as in Beringer et al. (2012) up to 200 g/cm^2 and is smaller at greater atmospheric depth, however, it is closer to the measurements of experiments. Finally, the results of electrons/positrons and pions are very close to the reference.

DYASTIMA also provides information about the energy, the direction and the arrival time of particles at each defined tracking altitude. Representative results at ground level are presented in Figs. 8–10. According to Fig. 8, which shows the energy distribution at sea level, it is resulted that the majority of muons have energies with magnitude 10^8 and 10^9 eV, while the majority of gammas have energy from 10^4 to 10^7 eV. Neutrons have a wide energy spectrum starting from thermal energies and reaching energies with magnitude 10^8 eV. Moreover, according to Fig. 9, which concerns the direction of the particles at sea level, muons have zenith angles from the vertical direction up to 60°, while the zenith angle of neutrons have a wide distribution with a maximum at about 40°. It is noticed that there is a portion of neutrons that have zenith angles greater than 90°, which means that they are moving upward. These neutrons are the result of elastic scatterings and have significantly lower energies (one to two orders of magnitude) compared to the neutrons that are moving downward. Finally, some results regarding the arrival time of particles are shown in Fig. 10. According to the left diagram of this figure, the arrival time of the neutrons at the ground is around 350 μs after the primary cosmic ray particles enter the atmosphere. However, there are neutrons with lower energies that delay and arrive at the sea level much later. The arrival time of the particles is correlated with their energy, as it can be noticed from the figure. The average arrival time of muons at each altitude is presented in the right diagram. A rough linear relation between the altitude and the arrival time is noticed.

Finally, a great feature of DYASTIMA is the provision of the spatial distribution of particles at each tracking altitude. This is very useful when monoenergetic beams are in focus, in order to study the dimension of the shower. Figs. 11 and 12 present the spatial distribution at several altitudes for the negative muons and neutrons respectively, when a vertical beam of 10 GeV protons enters the atmosphere. It is noticed that for the case of muons, the shower has a dimension of about 8×8 km at about 10 km altitude. Above and beyond this altitude the shower decreases and as a result it is much smaller at the surface. This happens because most muons are generated at about 15 km and decay as they travel downward or upward. Similar are the conclusions for the case of the neutrons, but the shower has a double dimension and is maximum at 16 km altitude. In the case of neutrons the shower forms a circle pattern due to the fact that the neutrons are not affected by the magnetic field.

4. Conclusions and future plans

In this work a new application named DYASTIMA that can be used for the simulation of atmospheric showers caused by the cosmic rays, is presented. The application is based on the Geant4 toolkit and aims to two main targets. The first target is the implementation of an easy to use application, while the second one is the provision of several output information that could fit to a variety of applications. The analysis and the results show that these two targets are fulfilled. On the first hand, DYASTIMA can easily be parameterized in several parts and the user can define a simulation scenario that fits his needs, concerning the primary cosmic ray spectrum, the atmospheric structure and the magnetic field. On the other hand, the output of DYASTIMA provides all the available information about the number, the energy, the direction and the arrival time of the secondary particles.

The first useful results of DYASTIMA have been presented and they can be summarized as follows:

- The peak of the secondary particle production appears at the altitude of 10–20 km.
- The majority of particles are electrons and gammas, however, a great portion of them has low energies due to ionization, Compton, photoelectric effect and Bremsstralung.
- Considering the vertical flux of particles with energies greater than 1 GeV, it is greater at an altitude of 16 km, while at sea level the most numerous particles are the neutrinos followed by muons and protons/neutrons.
- At sea level there are upward moving neutrons, as a result of elastic scatterings, which have significantly lower energies compared to the downward moving neutrons. All muons move downward with zenith angles up to 60°.
- Most neutrons arrive to sea level about 350 μs after the primary particles enter the atmosphere. About the muons, it is noticed a rough linear relation between the altitude and the average arrival time.

DYASTIMA is planned to be enhanced in the near future. The plans of this project can be distinguished in three axes. The first axis focuses on the application's user interface. Although the use of DYASTIMA is considered to be easy, the implementation of a graphical user interface in order to substitute the configuration files and make its usage even easier, is under consideration. The second axis focuses on the modeling of the atmosphere and the usage of the reference physics lists. The current modeling of the atmosphere does not take into account the small differences of the atmosphere's composition with altitude and the presence of humidity especially at the lower altitudes. These parameters will be considered in the next versions of DYASTIMA and will increase the accuracy of the results. Moreover, the first version of the application makes use of the Geant4 reference physics lists. Although these physics lists are validated by the high energy experiments and can be used in the case of cosmic rays, in our future plans is the implementation of a physics list especially for the simulation of cosmic rays in the atmosphere. Finally, the third and more important axis, concerns the extension of DYASTIMA with two more features. The first feature is the calculation of the equivalent dose in order for the application to be used for dosimetry applications. The second one is the use of the ground cosmic ray measurements (i.e. from the neutron monitors) for the automatic definition of the primary cosmic ray spectrum, used as input in the simulation. These two features will allow the use of DYASTIMA in a manner similar to AVIDOS (Latocha et al., 2009) and NAIRAS (Mertens et al., 2009) that calculate the radiation dose in which the air crews are exposed, by adapting the primary cosmic ray spectrum according to the ground based measurements of cosmic rays.

Acknowledgments

Athens Neutron Monitor station is supported by the Special Research Account of Athens University. L.I. Dorman thanks Israeli Ministry of Science for support in the frame of the project "National Centre of Knowledge in Cosmic Rays and Space Weather". Thanks also are due to Dr. John Apostolakis for his important advices and discussions about Geant4 toolkit.

References

Agostinelli, S., Allison, J., Amako, K., Apostolakis J. et al., 2003. for Geant4 collaboration: Geant4 – a simulation toolkit: NIM A, 506, 250.
Allison, J., Amako, K., Apostolakis, J., Araujo, H., et al., 2006. IEEE Trans. Nucl. Sci. 53, 270.
Apostolakis, J. et al., 2008. J. Phys.: Conf. Ser. 119, 032004.
Balabin, Yu.V., Gvozdevsk, B.B., Maurchev, E.A., Vashenyuk, E.V., Dzhappuev, D.D., 2011. Astrophys. Space Sci. Trans. 7, 283.
Banerjee, S. et al., 1999. Detector Description of CMS using Geant4, CMS Note.
Battistoni, G., Muraro, S., Sala, P.R., Cerutti, F., Ferrari, A., Roesler, S., Fasso, A., Ranft, J., 2007. AIP Conf. Proc. 896, 31.
Battistoni, G., Ferrari, A., Montaruli, T., Sala, P.R., 2003. Astropart. Phys. 19, 269, arXiv:hep-ph/0207035v2.
Belov, A., Eroshenko, E., Mavromichalaki, H., Plainaki, C., Yanke, V., 2005. Adv. Space Res. 35, 697.
Beringer, J. et al.for the Particle Data Group, 2012. Phys. Rev. 86, 010001.
Bütikofer, R., Flückiger, E.O., 2011. Astrophys. Space Sci. Trans. 7, 105.
Canadas, M., Arce, P., Rato Mendes, P., 2011. Phys. Med. Biol. 56, 273.
Clem, J.M., 1999. Atmospheric yield functions and the response to secondary particles of neutron monitors. In: Proc. 26th ICRC, vol. 7, 1999, p. 317.
Clem, J.M., Dorman, L.I., 2000. Space Sci. Rev. 93, 335.
Costanzo, D. et al., 2006. The Geant4-based simulation software of the ATLAS detector. Nuclear Science Symposium Conference Record, vol. 1. IEEE, p. 5.
Dartnell, L.R., Desorgher, L., Ward, J.M., Coates, A.J., 2007. Geophys. Res. Lett. 34 (2), 1–6. http://dx.doi.org/10.1029/2006GL027494, CiteID L02207.
Debrunner, H., Flückiger, E., Lockwood J., 1982. Specific yield function S(P) for a neutron monitor at sea level. In: Proc. 8th ECRS.
Desorgher, L., Flückiger, E.O., Gurtner, M., Moser, M.R., Bütikofer, R., 2005. Int. J. Modern Phys. A 20, 6802.
Desorgher, L., Flückiger, E.O., Gurtner, M., 2006. The PLANETOCOSMICS Geant4 application. In: 36th COSPAR Scientific Assembly, Meeting abstract from the CDROM, #2361.
Desorgher, L., Flückiger, E.O., Moser, M.R., Bütikofer, R., 2003. Geant4 simulation of the propagation of cosmic rays through the Earth's atmosphere. In: Proc. 28th ICRC.
Dorman, L.I., 2004. Cosmic Rays in the Earth's Atmosphere and Underground. Kluwer Academic Publishers.
Ferrari, A., Sala, P.R., Fasso, A., Ranft, J., 2005. FLUKA: a multi-particle, transport code, CERN-2005-10 (2005), INFN/TC_05/11, SLAC-R-773.
Flückiger, E.O., Moser, M.R., Bütikofer, R., Desorgher, L., Pirard, B., 2008. A parameterized neutron monitor yield function for space weather applications. In: Proc. 30th ICRC, vol. 1, p. 289.
Gaisser, T.K., Honda, M., Lipari, P., Stanev, T., 2001. Primary spectrum to 1 TeV and beyond. In: Proc. 27th ICRC, p. 643.
Gurtner, M., Desorgher, L., Flückiger, E.O., Moser, M.R., 2007. Adv. Space Res. 36, 2176.
Heck, D., Knapp, J., Capdevielle, J.N., Schatz, G., Thouw, T., 1998. CORSIKA: a Monte Carlo code to simulate extensive air showers. Forschungszentrum Karlsruhe GmbH, Karlsruhe (Germany), Feb 1998, V + 90 p., TIB Hannover, D-30167 Hannover (Germany).
Heikkinen, A., Boudard, A., Kaitaniemi, P., Folger, G., 2010. J. Phys.: Conf. Ser. 219. http://dx.doi.org/10.1088/1742-6596/219/3/032043, 032043 p.10.
International Association of Geomagnetism and Aeronomy, 2010. Geophys. J. Int. 183, 1216.
International Civil Aviation Organization. 1993. Manual of the ICAO Standard Atmosphere (extended to 80 kilometres (262 500 feet)), Doc 7488-CD, third ed.

Kaitaniemi, P., Boudard, A., Cugnon, J., Leray, S., Mancusi, D., 2010. on behalf of the Geant4 collaboration. INCL Intra-nuclear Cascade and ABLA De-excitation Models in Geant4. In: Proc. MC2010 Monte Carlo Conference.
Kobelev, P., Belov, A., Mavromichalaki, E., Gerontidou, M., Yanke, V., 2011. Variations of barometric coefficients of the neutron component in the 22–23 cycles of solar activity. In: Proc. 32nd ICRC.
Latocha, M., Beck, P., Rollet, S., 2009. Radiat. Prot. Dosim. 136 (4), 286.
Lockwood, J.A., 1971. Space Sci. Rev. 12, 688.
Longair, M., 2011. High Energy Astrophysics, 3rd ed. Cambridge University Press.
Matthiä, D., Heber, B., Reitz, G., Meier, M., Silver, L., Berger, T., Herbst, K., 2009. J. Geophys. Res. – Space Phys. 114, 2.
Maurchev, E.A., Gvozdevskij, B.B., Balabin, J.V., Vashenjuk, E.V., 2011. Modellig of hadron interactions in the neutron monitor. In: Physics of Auroral Phenomena, Proc. XXXIII Annual Seminar, Apatity, p. 83.
Mertens, C.J., Tobiska, W.K., Bouwer D., Kress, B.T., Wiltberger, M., Solomon, S.C., Murray J.J., 2009. Development of the nowcast of atmospheric ionizing radiation for aviation safety (NAIRAS) model, AIAA 2009-3633-978.
Miroshnichenko, L., 2001. Solar Cosmic Rays. Kluwer Academic Publishers.
Mishev, A.L., Usoskin, I.G., Kovaltsov, G.A., 2013. J. Geophys. Res.: Space Phys. 118, 2783.
Papaioannou, A., Mavromichalaki, H., Eroshenko, E., Belov, A., Oleneva, V., 2009. Ann. Geophys. 27, 1019.
Papini, P., Grimani, C., Stephens, S.A., 1996. Nuovo Cimento C Geophys. Space Phys. C 19, 367.
Paschalis, P., Mavromichalaki, H., Yanke, V., Belov, A., Eroshenko, E., Gerontidou, M., Koutroumpi, I., 2013a. New Astron. 19, 10.
Paschalis, P., Mavromichalaki, H., Dorman, L.I., 2013b. NIM A 729, 877.
Plainaki, C., Belov, A., Eroshenko, E., Kurt, V., Mavromichalaki, H., Yanke, V., 2005. Adv. Space Res. 35, 691.
Plainaki, C., Belov, A., Eroshenko, E., Mavromichalaki, H., Yanke, V., 2007. J. Geophys. Res. A 112, 4102.
Rodrigues, P., Moura, R., Ortigao, C., Peralta, L., Pia, M.G., Trindade, A., Varela, J., 2004. IEEE Trans. Nucl. Sci. 51, 1412.
Semikh, S., Serre, S., Autran, J.-L., Munteanu, D., Sauze, S., Yakushev, E., Rozov, S., 2012. IEEE Trans. Nucl. Sci. 59 (2), 303.
Shizake, Y. et al., 2007. Astropart. Phys. 28, 154.
Smart, D.F., Shea, M.A., Flückiger, E.O., 2000. Space Sci. Rev. 93 (1/2), 305.
Tsyganenko, N.A., 1989. Planet. Space Sci. 37, 5.
Tsyganenko, N.A., 1995. J. Geophys. Res. 100, 5599.
U.S. Government Printing Office. 1976. U.S. Standard Atmosphere, Washington D.C.
Usoskin, I.G., Kovaltsov, G.A., 2006. J. Geophys. Res. 111, D21206.
Usoskin, I.G., Gladysheva, O.G., Kovaltsov, G.A., 2004. J. Atmos. Solar-Terr. Phys. 66, 1791.
Usoskin, I.G., Kovaltsov, G.A., Mironova, I.A., 2010. J. Geophys. Res. 115, D10302.
Usoskin, I.G., Kovaltsov, G.A., Mironova, I.A., 2011. Numerical model of cosmic ray induced ionization in the atmosphere CRAC: CRII. In: 32nd ICRC, Beijing 2011, vol. 11, p. 344. http://dx.doi.org/10.7529/ICRC2011/V11/0284.